DOI: 10.24850/j-tyca-2025-01-03

Articles

Spatio-temporal trends in precipitation and temperature, as well as changes in Köppen-Geiger climate classes in the Sila river sub-basin, Mexico (1956-2015)

Tendencias espacio-temporales de precipitación y temperatura, así como cambios en clases climáticas de Köppen-Geiger en la subcuenca del río Sila, México (1956-2015)

Raquel Segundo-Sandoval[1], ORCID: https://orcid.org/0009-0007-9318-1355

Luis Ricardo Manzano-Solís[2], ORCID: https://orcid.org/0000-0002-6634-2930

Roberto Franco-Plata[3], ORCID: https://orcid.org/0000-0002-3031-6562

Víctor Hugo Guerra-Cobián[4], ORCID: https://orcid.org/0000-0001-6193-100X

[1]Faculty of Geography, Universidad Autónoma del Estado de México, State of Mexico, Mexico, rsegundos160@alumno.uaemex.mx

[2]Faculty of Geography, Universidad Autónoma del Estado de México, State of Mexico, Mexico, lrmanzanos@uaemex.mx

[3]Faculty of Geography, Universidad Autónoma del Estado de México, State of Mexico, Mexico, rfp@uaemex.mx

[4]School of Civil Engineering, Universidad Autónoma de Nuevo León, Nuevo León, Mexico, victor.guerracb@uanl.edu.mx

Corresponding author: Luis Ricardo Manzano-Solís, lrmanzanos@uaemex.mx

Abstract

According to various national and international institutions, which position Mexico as one of the most vulnerable countries to the effects of climate variability, such as extreme hydrometeorological events and climate change, with intensify some of these events. The research was conducted with the purpose of understanding how temperature and precipitation have behaved over a 60-year period (1956-2015), based on the analysis of monthly data from meteorological stations, using process automation (to structure geospatial data, perform interpolations, and classify climate according to Köppen-Geiger), and the use of geospatial tools, in one of the most important sub-basins as a source of drinking water supply, both for the region and for Mexico City, and one of the main agricultural areas in the State of Mexico. The results of the three analyses conducted in this study demonstrate that, although there have been some changes in precipitation and temperature values, these variations have not implied a change in the current climate type. However, it is not ruled out that this situation may be altered at the watershed level, as other authors assert, mentioning that precipitation is decreasing while temperatures are rising throughout the central region of the country. Therefore, integrated environmental conservation actions within the Sila river sub-basin are necessary to maintain current climatic conditions, thus safeguarding the well-being of future generations.

Keywords: Köppen-Geiger, Mann-Kendall, Sila river Sub-basin, Spatio-temporal analysis of change, TerrSet.

Resumen

De acuerdo con diversas instituciones nacionales e internacionales, México es uno de los países más vulnerables a los efectos de la variabilidad climática, como eventos hidrometeorológicos extremos y de cambio climático. La presente investigación se desarrolló con el propósito de conocer cómo se han comportado la temperatura y precipitación en un periodo de 60 años (1956-2015), a partir del análisis de los datos mensuales de las estaciones meteorológicas, mediante la automatización de procesos (para estructurar datos geoespaciales, hacer interpolaciones y clasificar el clima según Köppen-Geiger), y el uso de herramientas geoespaciales, en una de las subcuencas más importantes como fuente de abastecimiento de agua potable tanto para la región como para la Ciudad de México, y una de las principales zonas agrícolas del Estado de México. Los resultados de los tres análisis realizados en este estudio demuestran que aunque se han presentado algunos cambios en los valores de precipitación y temperatura, dichas variaciones no han implicado un cambio en el tipo de clima presente. Sin embargo, no se descarta que esta situación pueda verse modificada por cambios a nivel cuenca, como aseguran otros autores, quienes mencionan que la

precipitación está disminuyendo mientras que la temperatura está aumentando para todo el centro del país. Por lo tanto, se hacen necesarias acciones integradas de conservación ambiental dentro de la subcuenca del río Sila, que permitan mantener las condiciones climáticas actuales, salvaguardando así el bienestar de las futuras generaciones.

Palabras clave: análisis espaciotemporal del cambio, Köppen-Geiger, Mann-Kendall, Subcuenca del río Sila, TerrSet.

Received: 18/01/2023

Accepted: 08/09/2023

Published Online: 25/09/2023

Introduction

The United Nations Framework Convention on Climate Change (UNFCCC), in its first article, defines climate change as "climate change attributed directly or indirectly to human activity that alters the composition of the global atmosphere and that adds to natural climate variability observed over comparable time periods" (UN, 1992). Unlike climate change, climate variability is defined as variations in the average state of the climate. The term is used to indicate the deviations of the climatic statistics during a certain period of time (for example, a month, a season or a year), in comparison to the long-term statistics for the same calendar period according to World Meteorological Organization (OMM, following the Sppanish acronym) (OMM, 2022).

According to the Sixth Assessment Report (2023) provided by the Intergovernmental Panel on Climate Change (IPCC, 2023), an increase of 3.2 °C in the global average surface temperatures is projected by the year 2100 if the policies considered until the year 2020 do continue. Because of the increase in temperature on Earth, the hydrological cycle would be modified, since its movement is mainly due to the energy provided by the Sun to raise the water (evaporation) and to the terrestrial gravity that causes the evaporated water to descend in form of precipitation (rain or snowfall). These modifications could: 1) produce more intense and frequent rainfall (with risk of flooding); or, 2) reduce rainfall, generating drier summers (with risk of droughts).

Due to the above, authors such as Nigusie and Wondimagegn (2020); Fekadu, Biru and Mamo (2019); Nandi and Manne (2020); Nonki, Lenouo, Lennard and Tchawoua (2019); Pandey, Khare, Kawasaki and Mishra (2019), as well as Bedewi and Kumar (2018) consider that, due to climate change, water resources in arid or semi-arid regions such as Africa and India will decrease, which would mean that in the next 30 years, population living with water shortage could double. Instead, González-Celda, Ríos, Benegas-Negri and Argotty-Benavides (2021); Minga (2018); Pilares *et al*. (2018), in addition to Bedewi and Kumar (2018) predict an increase in the amount of rainfall, especially in countries such as Ecuador, Peru, Guatemala and Mexico, which could lead to extraordinary runoffs, so authors like Deng, Pisani, Hernández and Li (2020); Minga (2018); Pilares *et al*. (2018), and Vázquez-Ochoa, Correa-Sandoval, Vargas-Castilleja, Vázquez-Sauceda and Rodríguez-Castro (2021) interpret them as possible future risks that must be considered.

According to the Government of Mexico (Gobierno de la República, 2014), the country has geographical characteristics that place it as one of the most vulnerable countries to the effects of climate change. Its location between two oceans, its latitude and relief make it particularly exposed to different hydrometeorological phenomena (for example: droughts and hurricanes). Due to the high exposure of the Mexican territory, adaptation and mitigation to climate change is a priority. One way to start this process is by preparing a diagnosis of current and future vulnerability, which is the basis for the design and implementation of actions to reduce them. A fundamental aspect for the assessment of current and future vulnerability, within the process of adaptation to climate change, corresponds to the evaluation of climate variability (Conde & López, 2016).

This type of assessment must consider that neither climate variability nor climate change have a uniform behaviour over the territory (as can be misinterpreted when consulting small-scale or coarse-resolution maps on these issues), so they present differences depending on local conditions, being necessary to work with higher resolutions than those handled by the National Institute of Ecology and Climate Change (INECC, following the Spanish acronym) (INECC, 2022), who presents climate change scenarios for the entire country at a resolution of 30 km; however, such resolution is not enough to carry out a local analysis, nor for the identification of specific conservation, adaptation and/or mitigation strategies. The low resolution of these models is directly associated with the degree of uncertainty in climate projections, as they do not fully capture local variations. For example, with a 30 km resolution, the sub-basin would be contained within a single grid cell. This can lead to the interpretation that it is a homogeneous territory and that climate variability and/or change will behave uniformly across the entire sub-basin. Therefore, there is spatial uncertainty in this regard.

Specifically, the study area, which is the *Sila* river sub-basin, is located in the north of the State of Mexico. Its importance lies in the fact that it serves as a source of drinking water supply, not only for the region but also mainly for Mexico City (63 wells for urban public use and 91 wells for different uses) (State Commission for Natural Parks and Wildlife (Cepanaf, following the Spanish acronym) (Cepanaf, 2019); National Water Commission (Conagua, following the Spanish acronym) (Conagua, 2023); Rodríguez (2022), combined with the population growth and the demand for water, unplanned changes in land use, lack of piped water services, and high rates of marginalization in the upper parts of the sub-basin. Besides, inhabitants of the sub-basin have the perception that rainfall has decreased in recent years, causing damage to corn crops (Colaborador, 2020; Rodríguez, 2022) which are crucial for the indigenous-speaking population concentrated in the valley.

Taking these aspects into account, considering that up to now no studies of climate variability have been carried out in the *Sila* river sub-basin, with its possible consequences due to the change of climatic categories, it becomes essential to generate information that serves as a foundation for the analysis and interpretation of climate change scenarios, for the decisions that can be made based on them. Therefore, the development of this study answers the following questions: 1) How have precipitation and temperature behaved in the analysis along 60 years? 2) Has this behaviour involved changes in average weather conditions? 3)

Do the climate change scenarios in the area reflect the current trend? 4) Is this current trend accentuated or softened in the future?

For this purpose, literature related to the analysis of spatio-temporal trends was reviewed, highlighting the non-parametric Mann-Kendall method (Aawar, Khare, & Singh, 2019; Baig *et al*., 2022; Basarir *et al*., 2018; Krishnan, Prasanna, & Vijith, 2019; Marques *et al*., 2015; Nourani, Mehr, & Azad, 2018; Yanming, Jun, & Xinhua, 2011). Regarding the seasonal and transition/persistence analysis, Jiang, Xie, Zhao, He and He (2017); Ngoma, Wen, Ojara and Ayugi (2021), and Wang, Wang, Li, Wu and Yang (2015) point out that carrying out a climatic classification for two periods of time is the most concise way of observing the changes that have occurred between one stage and another. The Köppen climatic categorization modified by Geiger (hereinafter referred to as Köppen-Geiger) is one of the best-known climate classifications worldwide because it categorizes climates based on factors such as temperature and precipitation, generating categories that range from tropical to polar climates. This provides a comprehensive framework for understanding the climatic patterns of diverse regions (De Oliveira *et al*., 2020; Engelbrecht & Engelbrecht, 2016; Naranjo, Glantz, Temirbekov, & Ramírez, 2018; Rahimi, Laux, & Khalili, 2020; Ruman, 2020; Zeroual, Assani, Meddi, & Alkama, 2019).

Therefore, the objective of the research was to analyse the spatio-temporal and seasonal trends of the monthly climatic variables of precipitation and temperature, between 1956 and 2015, in the *Sila* river sub-basin, in Mexico, and their association with changes in the Köppen-Geiger climate classification, within the same period. Considering that the variables of temperature and precipitation directly affect the hydrological cycle (Aparicio, 1992; Brassington, 1988; Brooks, Ffolliott, & Magner, 2013; Campos, 1998; Campos, 2010; Chow, Maidment, & Mays, 1988; Davie, 2008; Heano, 2006; Linsley, Kohler, & Paulhus, 1958; McCuen, 1998; Shaw, Beven, Chappell, & Lamb, 2011; Viessman & Lewis, 1995), it was decided to evaluate them to meet the research objective.

The current investigation considered to analyse the data as spatio-temporal series of temperature and precipitation, to apply them to a trend analysis that will be complemented with the climatic classifications. These aspects are detailed in the following section.

Materials and methods

The *Sila* river sub-basin is located north of the State of Mexico and northwest of Mexico City. It has an approximate area of 638.22 square kilometers (km^2) and is located between the municipalities of *Ixtlahuaca*, *Jocotitlán*, *Atlacomulco*, *Morelos* and *Jiquipilco* (Figure 1), considered as indigenous peoples of the State of Mexico, according to the State Council for the Integral Development of Indigenous Peoples (CEDIPIEM, following the Spanish acronym) (CEDIPIEM, 2022). The main access roads to these municipalities are the Federal Highway 55D *Atlacomulco-Toluca* and the *Jilotepec-Ixtlahuaca* highway.

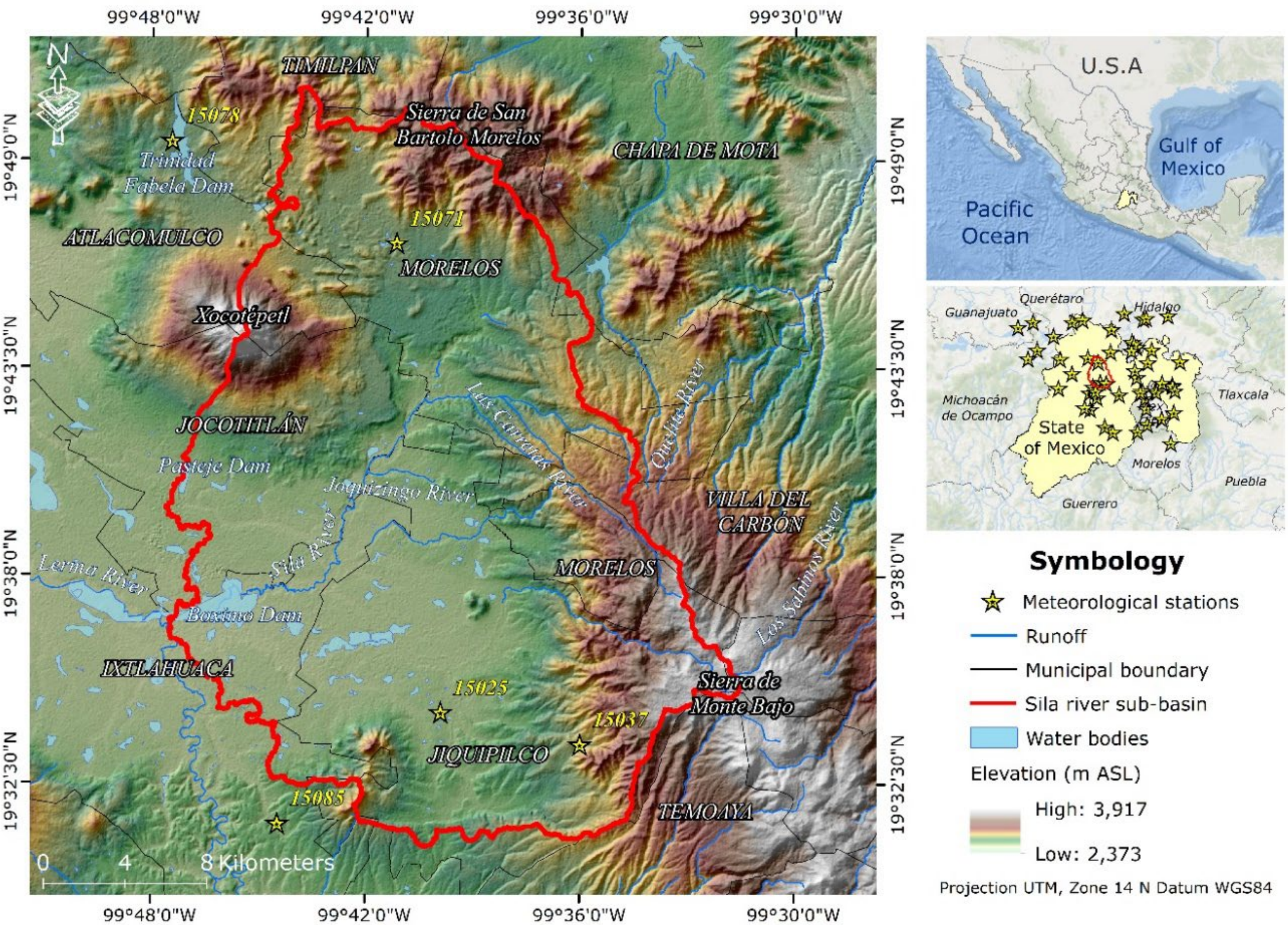

Figure 1. Location of the study area. Source: Own design based on data from the National Geostatistical Framework, INEGI (2020).

In general terms, the climate in the Sila river sub-basin, according to the Köppen-Geiger classification, is temperate, with warm summers, summer rainfall, and dry winters. As for the predominant land use in this area, rainfed agriculture stands out (INEGI, 2022), followed by irrigated agriculture; consequently, the primary use of surface water is directed toward agricultural activities. The population in the sub-basin has experienced an increase, growing from 88 720 inhabitants in 1990 to 158 708 inhabitants in 2020 (INEGI, 2020). The indigenous population is concentrated in the central-southern part of the sub-basin, whereas dwellings without access to piped water are located on the slopes of the sub-basin, close to the dividing line.

The main inputs for this research were daily data of precipitation and temperature (in millimeters and Celsius degrees, respectively), which were obtained from the Climate Computing project (CLICOM) of the National Meteorological Service (NMS). The stations inside and outside the *Sila* river sub-basin were considered, with data for the period 1956-2015 (Table 1). The mean temperature was obtained by averaging the minimum temperature and the maximum temperature, following the recommendation of the OMM (2018).

Table 1. Meteorological stations used for precipitation and temperature data.

ID	Latitude	Longitude	Years
9020*	19.297	-99.182	1956-2015
9022*	19.134	-99.173	1961-2015
9029	19.477	-99.091	1956-2015
9032*	19.191	-99.022	1956-2015
9043	19.465	-99.079	1956-2015
9048	19.404	-99.196	1956-2015
11012	20.198	-100.363	1962-2015

Tecnología y Ciencias del Agua
OPEN ACCESS

ID	Latitude	Longitude	Years
11031	20.143	-100.519	1957-2015
13018	20.229	-99.215	1956-2015
13025	20.239	-99.184	1961-2012
13060	20.265	-98.958	1956-2015
13064	20.289	-99.411	1963-2015
13068	19.936	-99.284	1956-2015
13075	19.99	-99.332	1956-2015
13084	19.964	-99.312	1956-2015
13089	19.898	-99.337	1956-2013
15008	19.544	-98.913	1961-2014
15010	19.462	-99.776	1961-2015
15020*	19.258	-98.896	1961-2015
15024	19.886	-99.555	1956-2015
15025	19.573	-99.665	1963-2015
15028*	19.909	-99.126	1961-2015
15037	19.559	-99.6	1962-2015
15038	19.051	-99.532	1956-2015
15041	19.562	-99.019	1961-2015
15055*	19.784	-98.832	1964-2015
15057	19.443	-99.464	1961-2015
15059	19.478	-99.221	1961-2015
15063	19.411	-99.699	1961-2015
15064	20.12	-99.544	1961-2015
15066	19.508	-100.098	1958-2015

ID	Latitude	Longitude	Years
15069*	20.219	-99.846	1961-2015
15071	19.78	-99.686	1961-2015
15073	19.623	-99.282	1961-2015
15074	19.695	-99.302	1961-2015
15076	19.663	-99.958	1961-2015
15078	19.825	-99.791	1961-2015
15083	19.532	-98.911	1961-2015
15085	19.524	-99.741	1964-2015
15086	19.476	-99.714	1961-2015
15089	19.292	-99.768	1956-2015
15108	19.306	-99.825	1962-2015
15115	19.775	-99.167	1961-2015
15122	19.107	-99.617	1959-2015
15127*	19.466	-99.246	1961-2015
15128	19.812	-100.081	1961-2015
15170	19.485	-98.886	1956-2015
15190	20.198	-99.956	1956-2015
16061	19.816	-100.416	1956-2015
16111	19.908	-100.319	1956-2015
16124	20.051	-100.149	1956-2015
17001	18.937	-98.928	1956-2014
17047	19.058	-99.274	1961-2015

*The station only had precipitation data.

It is important to mention that some of the stations had data from previous or subsequent years, but an effort was made to achieve a homogeneous distribution over the territory and with respect to the period of analysis. This reduced the number of stations to those that best matched a specific period, resulting in the period 1956-2015. It is also worth noting that, at the time of writing this document, the national database of the NMS was updated until the year 2020 (https://smn.conagua.gob.mx/es/climatologia/informacion-climatologica/informacion-estadistica-climatologica), but in practice, only some stations in the study area had complete data up to 2017.

Considering the previous criteria, these stations were excluded. To ensure the representativeness of precipitation and temperature data, the following steps were taken in each meteorological station: first, outliers and missing data were removed. Subsequently, the data sufficiency criterion of the OMM (2018) was applied as follows: to consider a month, it should have at least 80 % of days with data available; to consider a year, it should have at least 80 % of months with data for that year; and to consider station data, it should have at least 80 % of the years within the 1956-2015 period. This criterion further reduced the number of available stations because some stations had data within the selected period, but the data were incomplete, leading to their exclusion.

Subsequently, the point data of the stations were interpolated to generate monthly images of the continuous surface, using the ANUSplin software (Hutchinson & Xu, 2013), which interpolates using the thin-plate spline interpolation method that adjusts the smoothing parameters to the coordinates of longitude, latitude, and elevation of the geographic space. The interpolation uses Equation (1):

$$z_i = f(x_i) + b^T y_i + e_i (i = 1, \dots, N) \quad (1)$$

Where:

x_i = d-dimensional spline vector of independent variables

f = unknown smoothing function of x_i

y_i = p-dimensional vector of independent covariates

b^T = unknown p-dimensional vector of coefficients of y_i

e_i = zero mean error independent term

To perform the interpolation, ANUSplin requires latitude, longitude, and elevation data for each station to be processed. The latitude and longitude were taken from the CLICOM database, while the elevation was obtained from the Digital Elevation Model (DEM), as recommended by Hutchinson and Xu (2013). The resolution chosen as the baseline was ~30m, which is the one corresponding to the elevation numerical model obtained from the United States Geological Survey (USGS).

The process of obtaining elevations was automated using Object Pascal programming language in Lazarus and spatial analysis processes in TerrSet. Additionally, the creation of the annual input files required by ANUSplin to process each climatic element (precipitation and temperature) was automated. Each file contains, for each station and year, an identifier, longitude, latitude, elevation, and data for the 12 months of the year for interpolation.

The results were 720 raster layers, for each of the climate elements for the period 1956-2015 (Figure 2), at a resolution of 30 meters. As a result of the interpolation, annual weighted metrics Mean Error (ME), Mean Absolute Error (MAE), and Root Mean Square Error (RMS) were also obtained. These averaged values for the study period are presented in Table 2. The 2 880 raster layers obtained comprised the spatio-temporal series used in later stages, referring to a set of observations recorded at different times and locations, which provides a dataset that expresses spatial and temporal evolution.

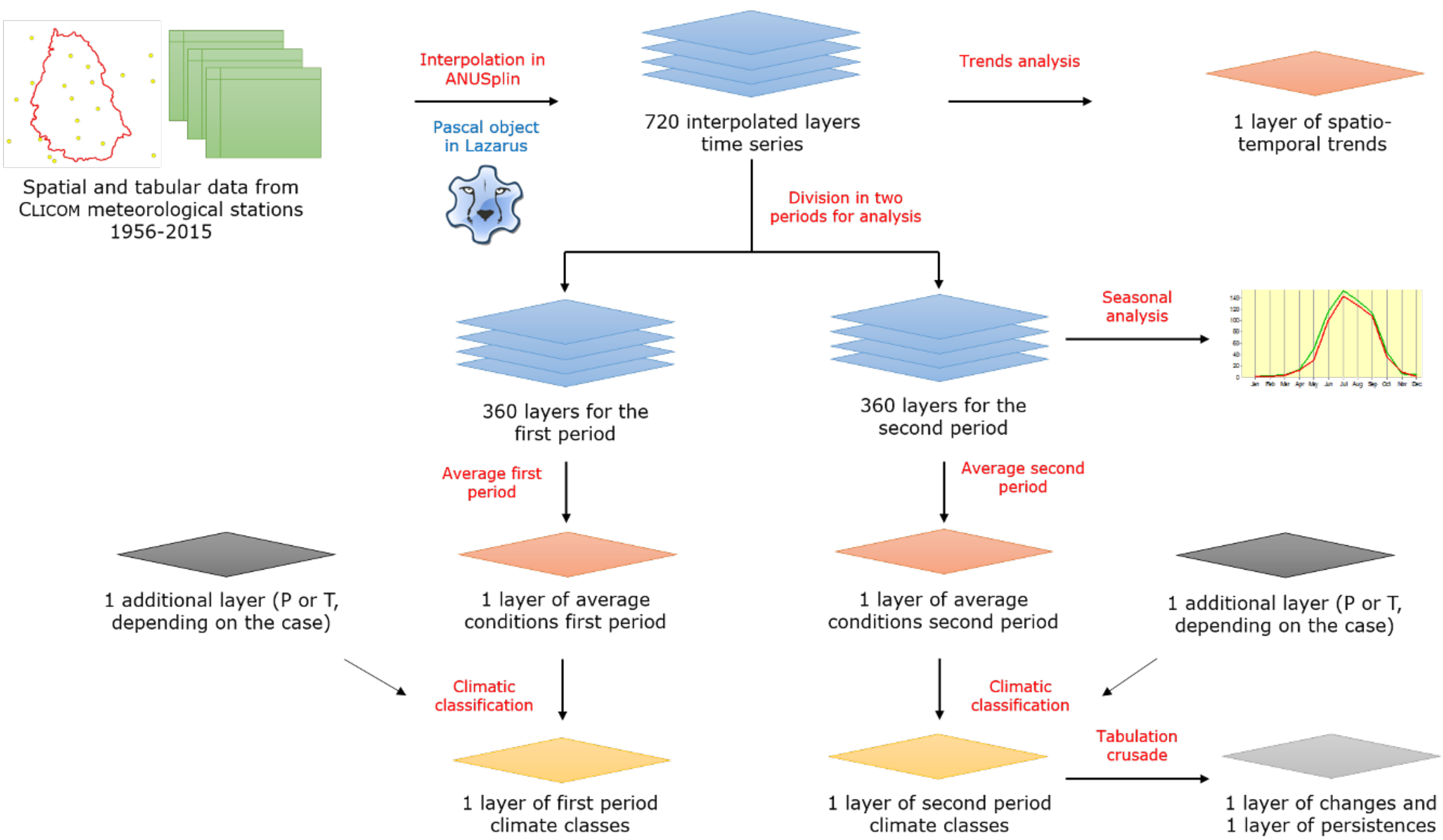

Figure 2. Data processing of precipitation (P) and temperature (T).

Table 2. Average of the annual metrics over the study period to assess the error in the interpolations.

Element	Criteria	ME	MAE	RMS
Precipitation (mm)	Maximum	-0.422	33.300	94.900
	Minimum	-4.970	13.800	24.400
	Average	-2.157	21.048	40.570
Maximum temperature (°C)	Maximum	0.372	2.240	3.440
	Minimum	-0.525	1.030	1.310
	Average	0.013	1.548	2.209
Mean temperature (°C)	Maximum	0.117	1.540	2.320
	Minimum	-0.309	0.831	1.120
	Average	0.005	1.149	1.571
Minimum temperature (°C)	Maximum	0.121	2.170	3.420
	Minimum	-0.112	1.120	1.570
	Average	0.009	1.448	1.995

First, the analysis of the spatio-temporal trend was conducted by applying the Mann-Kendall method (Ronald, 2016) to the seasonally adjusted series in the TerrSet software. Mann-Kendall allows identifying the presence of change trends and the degree to which they occur, which was used to show spatio-temporal trends of increases or decreases in precipitation and temperature: maximum, mean, and minimum (Equation (2)):

$$S = \sum_{k=1}^{n-1} \sum_{j=k+1} [\![sign(x_j - x_k)]\!] \quad (2)$$

Tecnología y ciencias del agua, ISSN 2007-2422, 16(1), 84-137. DOI: 10.24850/j-tyca-2025-01-03

x_j = ordered data values

n = length of the observations

S = Mann-Kendall statistics

The sign or signal of change of the statistical test is (Equation (3)):

$$sign(x_j - x_k) = \begin{Bmatrix} +1\ if\ x_j - x_k > 0 \\ 0\ if\ x_j - x_k = 0 \\ -1\ if\ x_j - x_k < 0 \end{Bmatrix} \quad (3)$$

for $n \geq 10$, then the statistics S has an approximately normal distribution, with mean zero ($E(S) = 0$) and variance as in the Equation (4):

$$V(S) = \frac{n(n-1)(2n+5) - \sum_{k=1}^{nk} t_k(k)(k-1)(2k+5)}{18} \quad (4)$$

t_k = number of links or duplicates in measure k.

Equation (3) is used in case of tied values of time series.

nk = total number of links in the data set

In case of having $n \geq 10$, the standardized test statistics for Mann-Kendall can be calculated using Equation (5):

$$Z_s\begin{Bmatrix}\frac{S-1}{\sqrt{v(s)}} & (if\ S>0)\\ 0 & (if\ S=0)\\ \frac{S+1}{\sqrt{v(s)}} & (if\ S<0)\end{Bmatrix} \quad (5)$$

The probability density function for a normal distribution with a mean of 0 and a standard deviation of 1 is expressed by Equation (6) (U.S. Army Corps of Engineers, 2005):

$$f(z)=\frac{1}{\sqrt{2\pi}}e^{-\frac{z^2}{2}} \quad (6)$$

For this research, a significance level of 95 % probability was used. To make the final categorization, U.S. Army Corps of Engineers' criterion (2005) was adopted, which indicates that a trend is decreasing if Z is negative and the calculated probability is greater than the significance level; whereas the trend is increasing when Z is positive and the calculated probability is greater than the significance level; finally, there is considered to be no trend when the calculated probability is less than the significance level.

Subsequently, TerrSet's Earth Trend Modeler (ETM) (Ronald, 2016) was used to perform the seasonal analysis, to expose possible seasonal lags and variations in the monthly amounts of climatic elements. In this case, each 60-year monthly series was divided into two 30-year series each, to compare the interannual monthly behaviour of both series, with the purpose of identifying the beginning and early end of the rainy and warm seasons, as well as their start and/or late completion. Likewise, increases or decreases in the monthly values of one period compared to the other were identified and quantified using the Nash-Sutcliffe coefficient (Diaz, Bâ, Quentin, Ortiz, & Gama, 2015) as shown in Equation (7). The value of this coefficient is 1 when the values of the two series are identical, and as the difference between these series increases, this coefficient decreases and can even become negative:

$$Nash = 1 - \frac{\sum_{i=1}^{n}(P1_i - P2_i)^2}{\sum_{i=1}^{n}(P2_i - \overline{P2})^2} \quad (7)$$

Where:

$P1_i$ = value of month i in the first period

$P2_i$ = value of month i in the second period

$\overline{P2}$ = average of the monthly values in the second period

For the Köppen-Geiger analysis, the monthly precipitation and temperature values of the raster layers were averaged for each month, considering two periods, one from 1956 to 1985 and another from 1986 to 2015, to represent the average condition of 30 years in each. For each of these periods, the Köppen-Geiger climatic classification was carried out. This classification was carried out in TerrSet, using the module developed by Colín (2021). Subsequently, the TerrSet module (LCM) was used to model changes in climatic categories, specifically through the cross-tabulation tool, to identify areas of the sub-basin with transitions and persistence in the climatic categories, between the periods analysed. With these results, it was possible to characterize the most significant transitions.

Tecnología y Ciencias del Agua
OPEN ACCESS
Check for updates

Results

Spatio-temporal trends analysis

To interpret the results of the Mann-Kendall analysis for precipitation and temperature of the seasonally adjusted series, it is important to take into consideration the thresholds and implications shown in Table 3 and Table 4.

Table 3. Values and implications of the Mann-Kendall trend analysis (S).

Values	Implications
$-1 \leq S < 0$	Trend towards decreasing values
$S = 0$	Absence of trend.
$0 < S \leq 1$	Trend towards increasing values.

Table 4. Criterion used in TerrSet to categorize Mann-Kendall trends.

Normalized test statistic *Z*	Logical operator for overlay in TerrSet	Probability (*p*) versus level of significance (0.95)	Trend
$Z < 0$	AND	$p \geq 0.95$	Decreasing
$Z > 0$	AND	$p \geq 0.95$	Increasing
$Z = 0$	OR	$p < 0.95$	No trend

Source: Self-prepared based on HydroGeoLogic-U.S. Army Corps of Engineers (2005).

It is worth mentioning that the analysis of spatio-temporal trends was carried out for the study area and the periphery, but the interpretation of the values of all the results refers only to the area within the sub-basin.

For the specific case of precipitation, the trend values are between -0.014 and -0.089 (Figure 3). Although these numbers are negative, they remain close to zero, which does not imply a significant downward trend, indicating that the precipitation values have remained stable through the last 60 years of monthly records. Regarding the maximum temperature, the trend values are between 0.060 and -0.480 (Figure 4). The first is a value very close to 0, indicating that there is no tendency for maximum temperature to increase or decrease, while the second one shows a moderately significant decrease from the center to the northeast of the sub-basin.

Tecnología y Ciencias del Agua
OPEN ACCESS
Check for updates

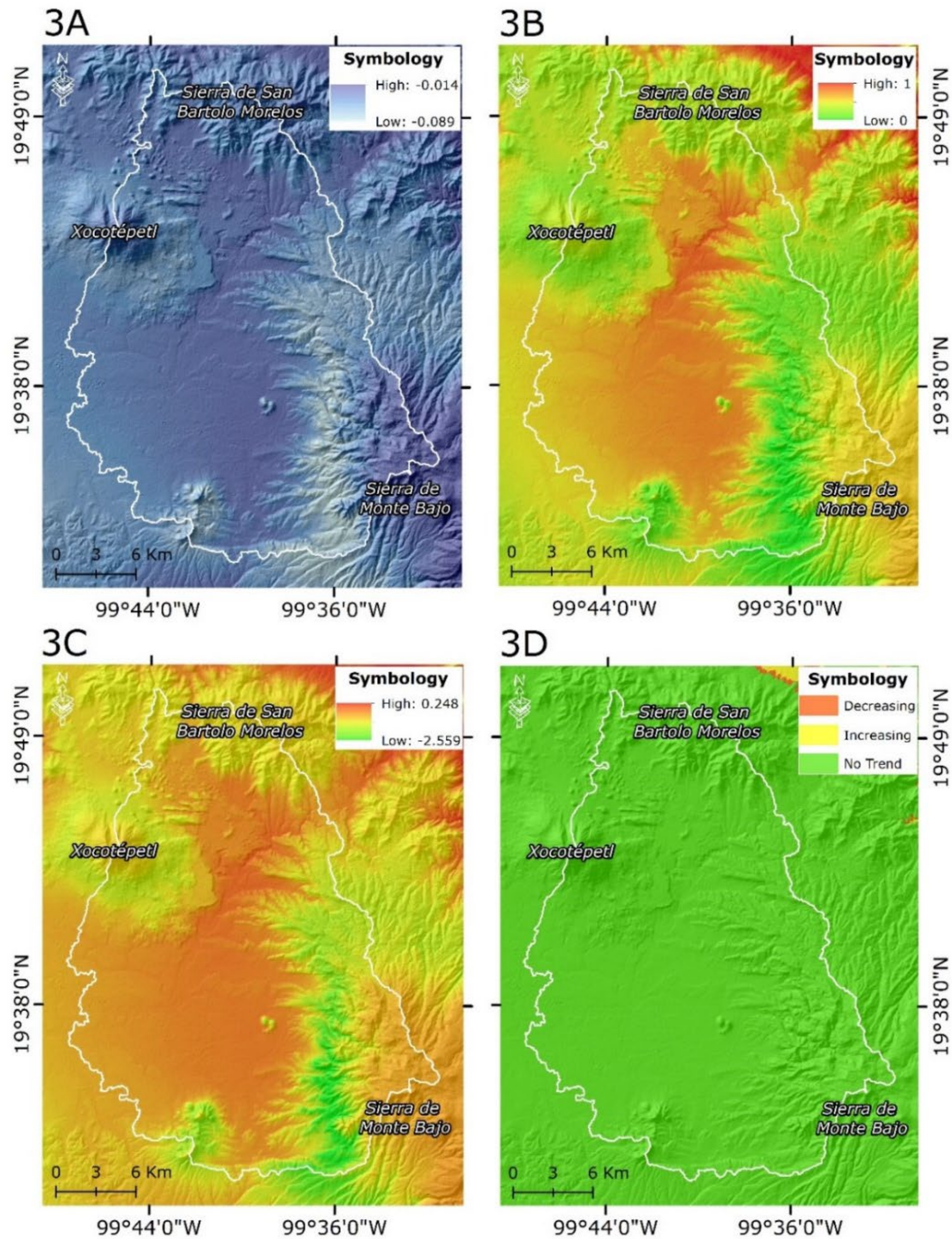

Figure 3. Spatio-temporal trend analysis for monthly precipitation (1956-2015): 3a, Mann-Kendall (S); 3b, probability; 3c, normalized test statistic (Z); 3d, trend (at 95 % level of significance).

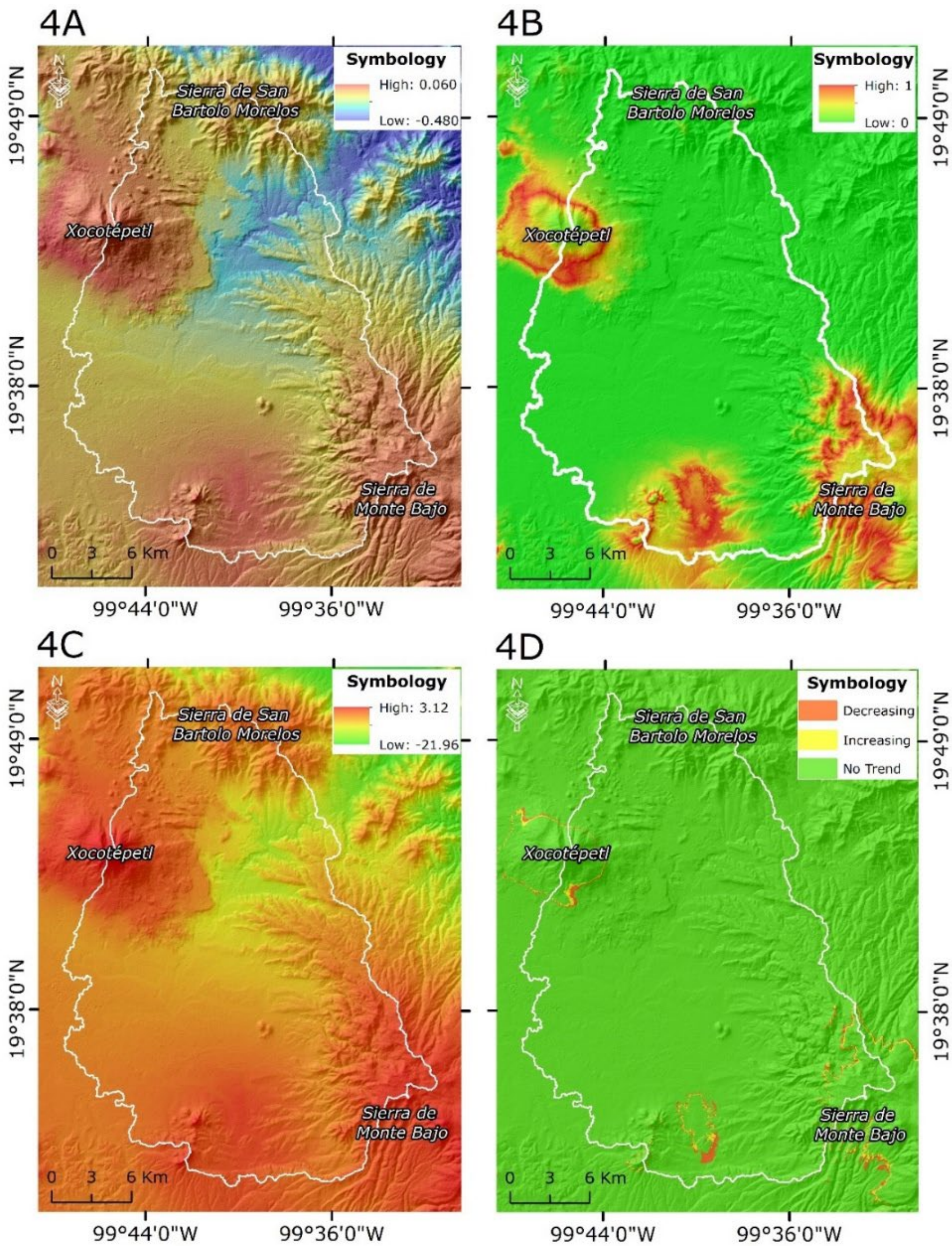

Figure 4. Spatio-temporal trend analysis for monthly maximum temperature (1956-2015): 4a, Mann-Kendall (S); 4b, probability; 4c, normalized test statistic (Z); 4d, trend (At 95 % level of significance).

Regarding the mean temperature, the trend values are between -0.033 and -0.436 (Figure 5). Although the first is a negative value that remains close to zero, the second one shows a moderately significant decreasing trend from the center to the northeast of the sub-basin (as happens with the maximum temperature trend values). Finally, and in the case of the minimum temperature, the trend values are between 0.019 and -0.092 (Figure 6). Although one is positive and the other negative, both values are very close to zero, which indicates that there is no significant trend of increasing or decreasing the minimum temperature in the sub-basin.

Tecnología y Ciencias del Agua
OPEN ACCESS
Check for updates

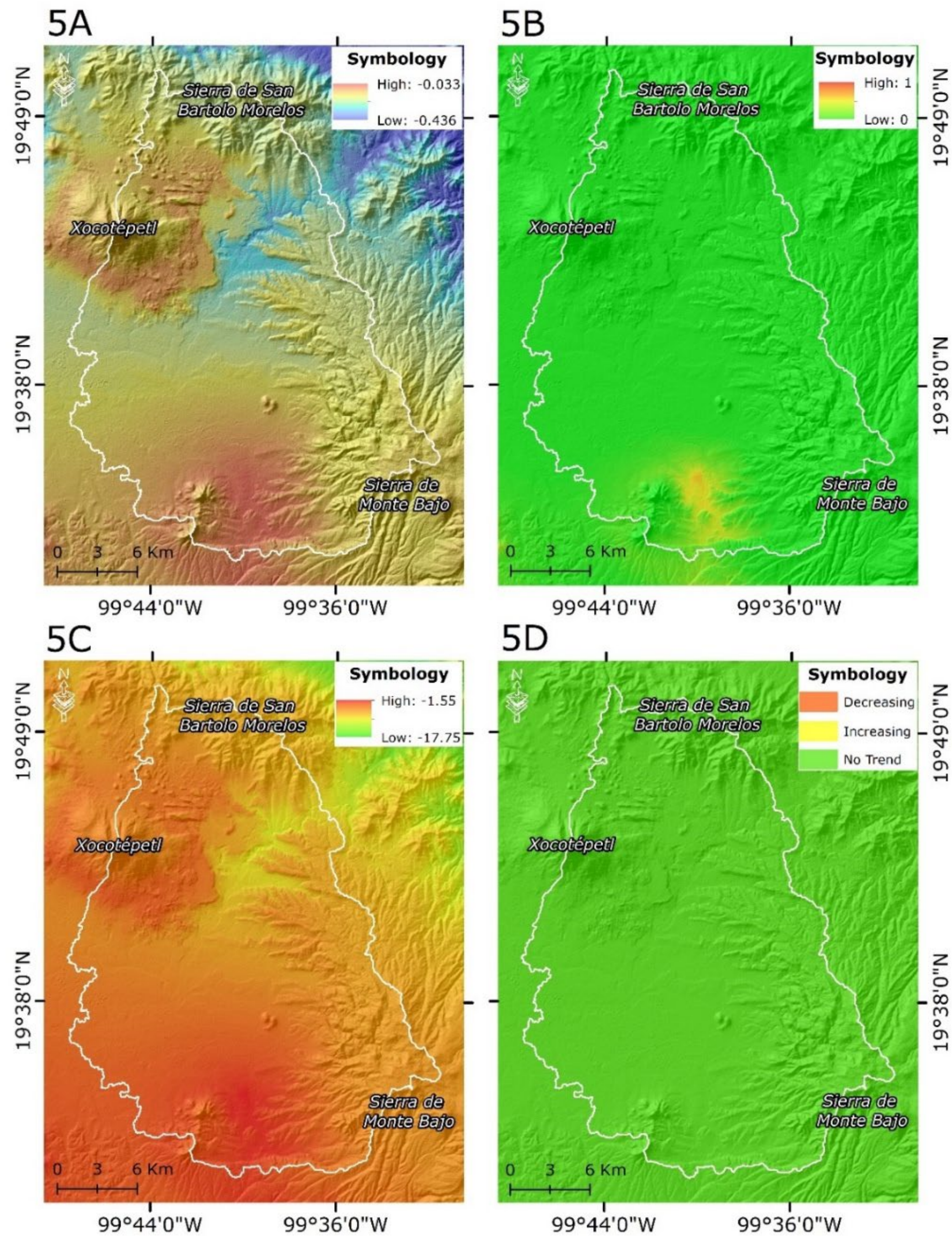

Figure 5. Spatio-temporal trend analysis for monthly mean temperature (1956-2015): 5a, Mann-Kendall (S); 5b, probability; 5c, normalized test statistic (Z); 5d, trend (at 95 % level of significance).

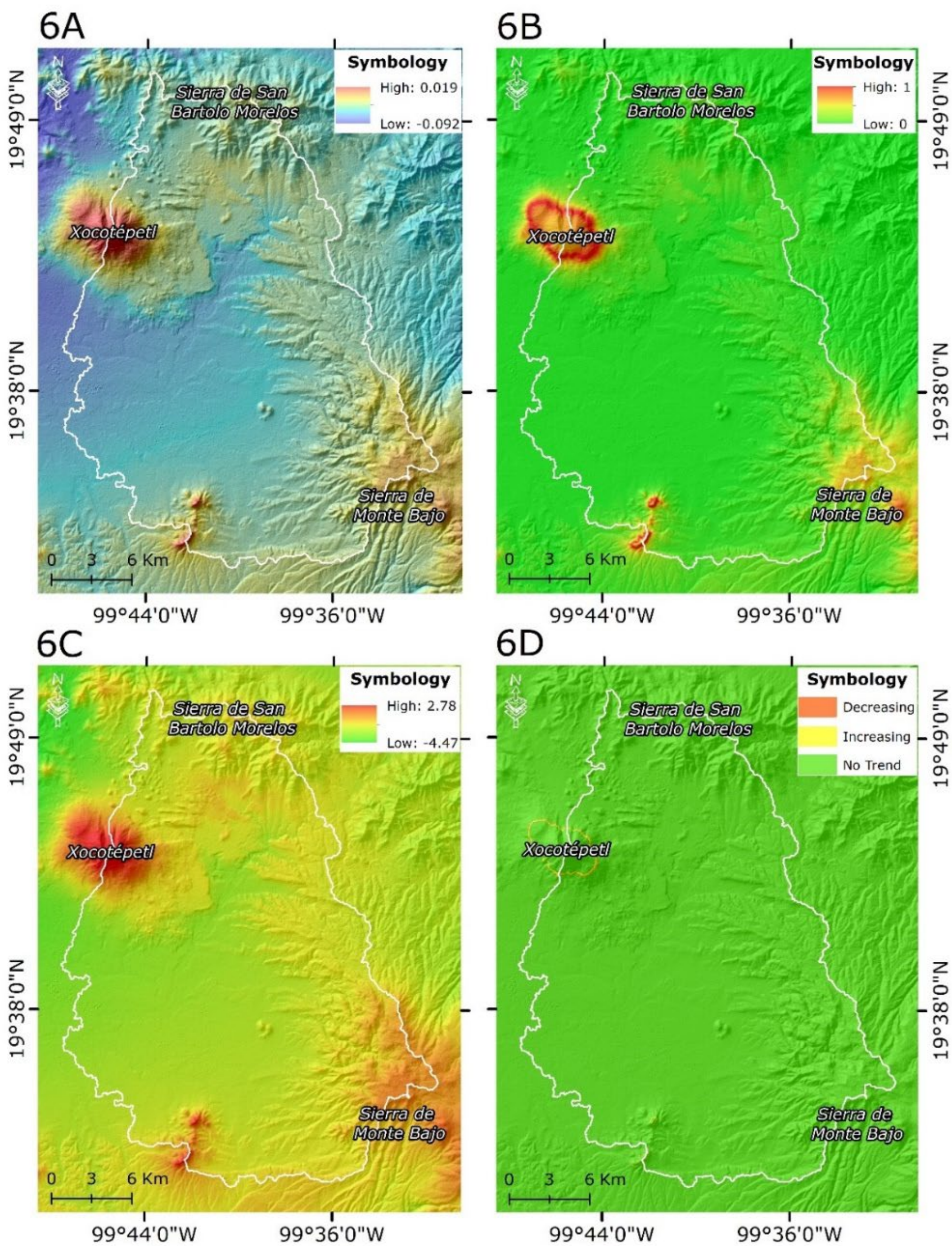

Figure 6. Spatio-temporal trend analysis for monthly minimum temperature (1956-2015): 6a, Mann-Kendall (S); 6b, probability; 6c, normalized test statistic (Z); 6d, trend (at 95 % level of significance).

Therefore, although S values were presented below and above zero in maximum, mean and minimum temperatures, these values do not represent a decrease or increase trend in temperature in the *Sila* river sub-basin, because they remain closer to zero than to -1 or 1, which indicates that they are not very significant or moderately significant in some areas.

Taking into account categories in Table 4, it is evident that precipitation, minimum temperature and mean temperature do not express any trend in the sub-basin (Figure 3d, Figure 5d and Figure 6d), and only maximum temperature shows small zones with trends to decrease or increase, but it is mainly evident the lack of trend to change (Figure 4d).

Considering the climatic elements analysed (precipitation and maximum, mean and minimum temperature) at a monthly level, within the period 1956-2015, it can be established that the sub-basin shows a condition of climatic stability. This statement is strengthened with the seasonality analysis and with the analysis of transition/persistence among climatic categories.

Seasonal analysis of amplitude and frequency

The main purpose of this analysis was to know the seasonal behaviour of the climatic elements analysed (precipitation, temperature maximum, mean and minimum) and their differentiation in terms of the beginning and end of both the rainy season and the warm season, as well as the difference of the monthly values of precipitation and temperature that exist within the first period (1956-1985) and second period (1986-2015) of analysis. The results are shown in Figure 7. The first period is represented by a green line and the second period by a red line. In order to assess the overall behaviour between one period and another, Figure 7 shows the Nash coefficient. In all cases, this coefficient indicates that the two series are very similar according to the criteria of Da Silva, Araujo and Fábio (2022), as the coefficients were above 0.9.

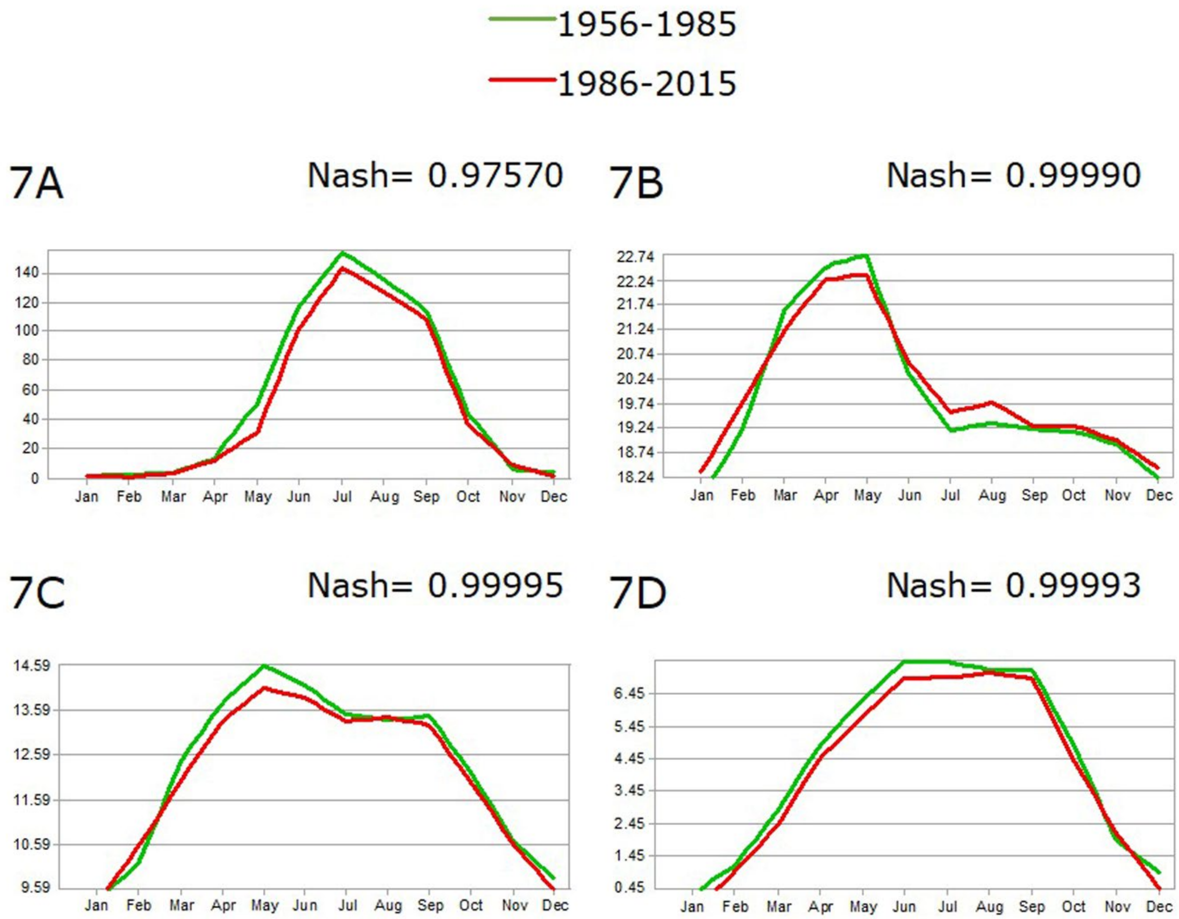

Figure 7. Seasonal analysis of amplitude and frequency (1956-2015): 7a, monthly total precipitation; 7b, average of monthly maximum temperature; 7c, average of monthly mean temperature; 7d, average of monthly minimum temperature.

Regarding the behaviour of monthly total precipitation, Figure 7a shows that the rainy season is kept between the months of May to October, that is, in both cases it is a summer rain regime. Regarding the amount of total precipitation in each month, the graph shows higher values in the first period 1956-1985, compared to the second period

1986-2015. The main difference is observed in the month of May, since, for the first period, the monthly total precipitation was 55 mm and for the second, 35 mm, showing a reduction of 20 mm between one period and another. The month of July was the rainiest month in both cases, with values of 153 mm and 144 mm for the first and second periods, respectively. Despite these differences, the analysis of the climatic categorization presented in the following section indicates that these changes in monthly precipitation values have not modified the type of climate present in the sub-basin.

Regarding the average of the maximum temperature for each month (Figure 7b), two aspects stand out: the first is that there is a warmer season (March to June) and a less warm season (July to February). The second aspect is that, in the warmer season, the first period of analysis (1956-1985) was higher than the second (1986-2015), while in the less warm season, the opposite occurs. In the warmer season, the highest value occurs in the month of May in both periods, being 22.7 °C in the first period and 22.3 °C in the second period. Regarding the less warm season, the highest value occurs in the month of August, being 19.4 °C in the first period and 19.8 °C in the second period, showing a difference of 0.4 °C in both cases.

About the average of mean temperature for each month (Figure 7c), in most months, the values of the first period (1956-1985) remained above the values of the second period (1985-2015), with May being the month with the highest temperatures, 14.6 °C for the first period and 14.1 °C for the second period. It was also the month in which the greatest differentiation (0.5 °C) occurs between one period and another.

The last result of this section is the average of minimum temperature in each month. From the temporal point of view, the warm season begins later and ends earlier in the second period (Figure 7d), but in both cases, there is a maximum difference of six days. Comparing one period to another, most of the values were higher in the first period. Specifically, the most significant differences are shown from March to July. The greatest differentiation of values is shown in June and July, being in both cases 7.4 °C and decreasing 0.5 °C in the second period.

Considering the periods 1956-1985 and 1986-2015, it can be observed that for the monthly averages of maximum temperature, a difference of 0.4 °C is noticeable between the warmest and least warm stations. Meanwhile, for the monthly averages of mean and minimum temperatures, the difference was 0.5 °C. Despite these differences expressed in temperature, between one period and another, the type of climate has not changed in the sub-basin, according to the analysis of climate categorization presented in the following section.

For the second period of analysis (1986-2015), the values of total monthly precipitation were reduced in most of the annual period. The same happens with the average of the monthly mean and minimum temperatures. Regarding the average of the maximum temperature, the second period of analysis showed an increase from July to February (less warm season) and a reduction of values from March to June (warmer season). However, these indications of reduction and increase of values in the analysed climate elements are not evident, because they do not imply changes with respect to the type of climate present in the sub-basin, as explained in the next section.

Climate category transition analysis

The Köppen-Geiger climate classification was carried out to represent the average conditions of 30-year periods, the first one spanning from 1956 to 1985, and the second from 1986 to 2015 (Figure 8, as well as in Table 5). The results of the climatic classification for the first period (1956 to 1985) show that, in general terms, there are two types of climates: temperate climate (*C*) and tundra climate (*E*). The first one varies from a warm temperate climate, with dry winters and hot summers (*Cwb*), which is the predominant one, followed by the warm temperate climate with dry winter, cool summer, and cold winter (*Cwc*), which is expressed in the foothills of *Xocotépetl* and *Sierra de Monte Bajo*. For the first period, the high mountain tundra climate (*ET*) is only present at the summit of *Xocotépetl*.

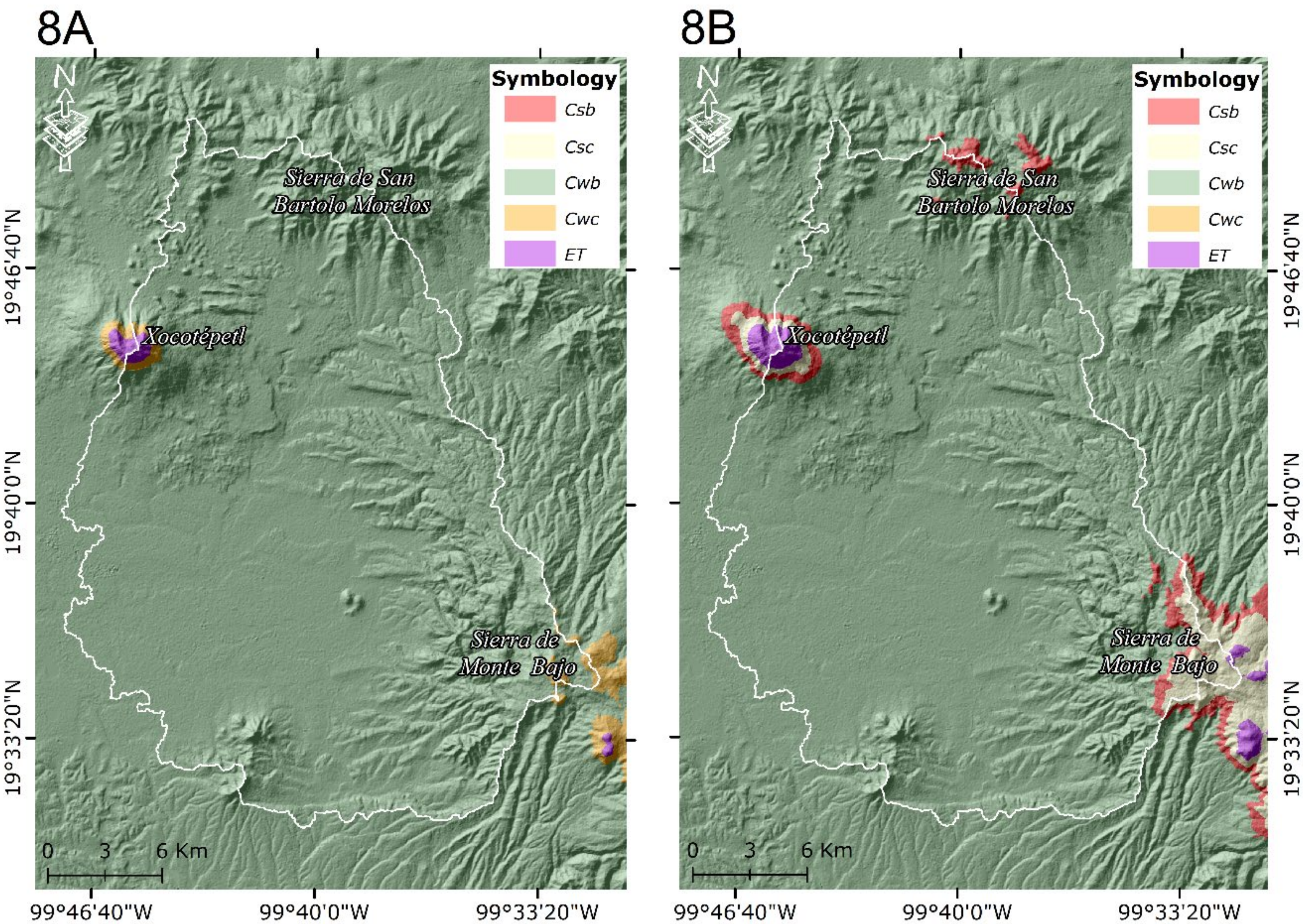

Figure 8. Köppen-Geiger climatic classification: 8a, first analysis period from 1956 to 1985, and 8b, second analysis period from 1986 to 2015.

Table 5. Climates present in the Sila river sub-basin in the last 60 years (1956 to 2015), according to the Köppen-Geiger classification.

Climate symbol	Climate description
Csb	Warm temperate climate with dry summer, hot summer
Csc	Warm temperate climate with dry summer, cool summer, and cold winter
Cwb	Warm temperate climate with dry winter, hot summer
Cwc	Warm temperate climate with dry winter, cool summer, and cold winter
E	Tundra climate
ET	High mountain tundra climate

The climatic classification of the second period (1986 to 2015) shows similar results to the first one. The two present climates are *C* and *E*. The predominant climate in the study area remained *Cwb*, and, according to the altitude of the zone, other varieties of the *C* climate were present, specifically warm temperate climates with dry summer and hot summer (*Csb*) in the lower foothills of the *Sierra de San Bartolo Morelos*, *Sierra de Monte Bajo*, and *Xocotépetl*, and the warm temperate climate with dry summer, cool summer, and cold winter (*Csc*) in the upper foothills of the same mountains. However, the *Cwc* climate disappeared for the second period, while the *ET* climate persisted and expanded a bit more in the highlands.

From the quantitative point of view, and according to the Köppen-Geiger climatic classification, 96.5 % of the total area of the sub-basin did not present any type of change in climate categories between the first (1956-1985) and second period (1986- 2015), as illustrated in Figure 9a, so most of the sub-basin remains in a warm temperate climate, with dry winters and hot summers (*Cwb*). In the areas where there was a change, that is, the remaining 3.5 %, it mainly refers to a transition between varieties of climate *C* (Figure 9b). What in the first period was *Cwb*, it changed to *Csb* by 1.5 % and it also changed to *Csc* by 1.5 %, representing a total change of 3 %. The other 0.5 % is divided between a 0.3 % change from *Cwc* to *Csc* in the *Sierra de Monte Bajo*, and a 0.2 % increase in *ET* in *Xocotépetl*.

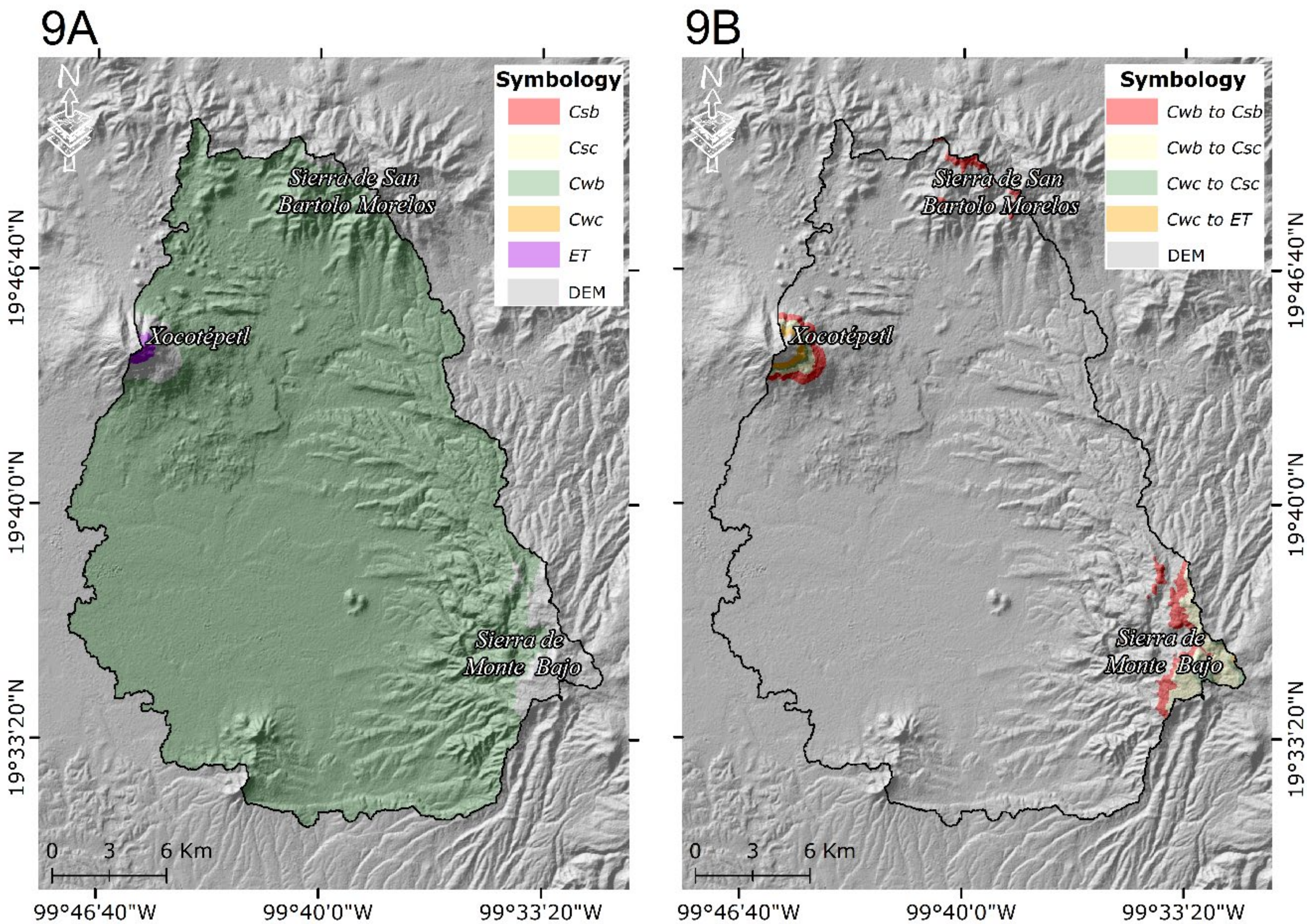

Figure 9. Transition and persistence in the Köppen-Geiger climate classification between the periods 1956-1985 and 1986-2015; 9a, persistence and 9b, transitions.

These changes in the varieties of climate *C* refer mainly to the rainfall regime (second letter), which changed from a rainfall regime with a dry winter (*w*) to one with a dry summer (*s*), from the first to the second period respectively. Regarding the behaviour of temperatures in summer (third letter), changes are only observed on the slopes of the *Sierra de Monte Bajo* and in *Xocotépetl*, going from cool summer (*c*) to hot summer (*b*). However, since these changes remain within climate *C* and only occur in 3.5 % of the sub-basin, -because the rest of the area (96.5 %) remains within the same classification (*Cwc*)-, they do not refer to a significant change in weather.

Therefore, considering the results of the Köppen-Geiger climate classification, warm temperate climates predominate around, both in the first and in the second period. In both cases, there is the presence of a tundra climate, without showing a significant change within the last 60 years.

The behaviour of absolute values can be observed in Figure 10, between the first period (1956-1985) and the second period (1986-2015), the tundra climate increased by 1.3 km², the Csb increased by 9.5 km², and the Csc increased by 11.7 km²; conversely, for the second period, the Cwc decreased by 3.6 km², and the Cwb decreased by 18.9 km².

Tecnología y ciencias del agua, ISSN 2007-2422, 16(1), 84-137. DOI: 10.24850/j-tyca-2025-01-03

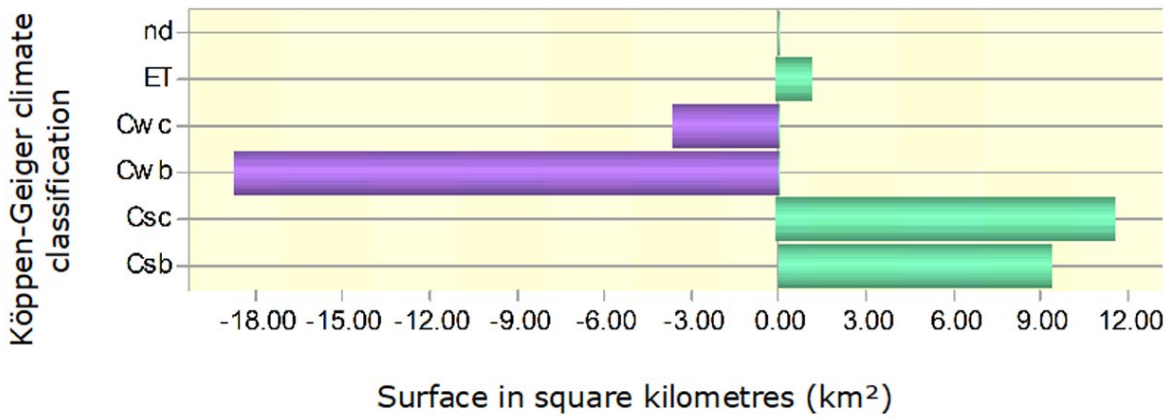

Figure 10. Losses and gains in the sub-basin between the first (1956-1985) and the second (1956-1985) period of analysis of the Köppen-Geiger categories.

Discussion

Based on the results of the Mann-Kendall spatio-temporal trend analysis, it was possible to establish that, although there are variations in the increase and decrease in precipitation, maximum, mean and minimum temperature, these variations do not indicate a significant trend (Figure 3, Figure 4, Figure 5 and Figure 6). The two climatic elements (precipitation and temperature) have remained constant within the *Sila* river sub-basin in the months of the period 1956-2015 (60 years). This statement is strengthened with the seasonal analysis of amplitude and frequency (Figure 7) and the analysis of transition/persistence between climatic categories (Figure 8, Figure 9, and Figure 10).

The seasonal analysis of amplitude and frequency of precipitation and temperature (maximum, mean and minimum) for the two 30-year periods (1956-1985 and 1986-2015) shows that both the rainy season (from May to October) and the warm season (from March to June) have not experienced changes and remain in the same months in both periods. Regarding the values of precipitation and maximum, mean and minimum temperatures, most of them were higher in the first period (1956-1985) compared to the second period (1986-2015); however, despite these differences, the current climate type in the sub-basin has not been modified according to the climate categorization analysis.

The results of the Köppen-Geiger climate classification of the first period and second period (1956 to 1985 and 1986 to 2015) show that, in general terms, there are two types of climates (directly related to the relief of the sub-basin): the temperate climate (*C*) and tundra climate (*E*), without showing a significant change in these 60 years. The first is distributed in most of the sub-basin, both in valleys and on slopes, while the second only occurs on the tops of the mountains in the area. Specifically, the current climate in 96.5 % of the total area of the sub-basin is temperate with dry winter and warm summer (*Cwb*); and in the area where changes in climate variables occur, the change primarily refers to the rainfall pattern (second letter), which shifted from a regime of rainfall with dry winter to one with a dry summer, from the first to the second period, respectively. Like what was obtained by Colín (2021) and reported by Karger *et al*. (2017), where they show that, in general, the entire area of the sub-basin, in the period 1981-2010, the climate is *Cwb* at a resolution of 1 km.

However, some other studies carried out for the State of Mexico and the central zone of the country affirm that precipitation has decreased and could continue to decrease in the coming years because of the effects of climate change. Such is the case of López *et al*. (2021), who mention that the average annual precipitation has decreased throughout the State of Mexico, as well as Núñez-González (2020), who carried out a trend analysis for the entire Mexican Republic, showing a reduction in the precipitations registered from 1960 to 2010 of northeast and central Mexico. However, these results have been obtained in a general way, both at the State level and at the country level, with annual data, and do not indicate whether this trend has had implications in the climate categories.

On the other hand, Astudillo-Sánchez, Villanueva-Díaz, Endara-Agramont, Nava-Bernal and Gómez-Albores (2017) report a reduction in summer precipitation and an increase in precipitation and winter temperature in some years from 1985 to 2012, dominated by warm conditions of *El Niño*. These results were obtained by analyzing the ring width of *Pinus hartwegii* that is in the forests of the Trans-Mexican Volcanic Axis, which shows a similar behaviour to that presented in the seasonal analysis of amplitude and frequency. In addition, these results could be closely related to the perception that the population has regarding the reduction in precipitation, especially attributed to the decrease in precipitation in May, a month that is related to the beginning of the rainy season (Bee, 2014).

Finally, it is important to indicate that the models of different climate change scenarios for Mexico suggest a decrease in precipitation and an imminent increase in temperature in the next 80 years, for the north of the State of Mexico (INECC, 2022). However, it's important to consider that these projections are made at an approximate resolution of 900 meters, which could lead to a generalization of global patterns in a local context.

Conclusions

A spatial-temporal trend analysis, a seasonal analysis, and a Köppen-Geiger climate category transition analysis were carried out in the *Sila* river sub-basin. The first was conducted for a 60-year period (1956-2015), using the non-parametric Mann-Kendall method to identify spatial-temporal trends of increases or decreases in precipitation and temperature (maximum, mean and minimum). The seasonal analysis of amplitude and frequency was performed for the same 60 years, divided into two 30-year periods (1956-1985 and 1986-2015), and was used to understand the behaviour and distribution in terms of the onset and end of rainy seasons, warmer and less warm seasons, as well as the difference in precipitation and temperature values within the first period (1956-1985) compared to the second period (1986-2015) of analysis. Finally, for these same 30-year periods (1956-1985 and 1986-2015), the Köppen-Geiger climate classification was carried out to identify the types of climates present in the sub-basin, and a transition/persistence analysis was conducted to identify how the climate categories of the two analysed periods have been modified.

The results served to address the research questions presented in the introduction. Therefore, according to the spatial-temporal trend analysis, the precipitation and minimum temperature values remained stable over the 60-year period of analysis. In terms of mean and maximum temperature, moderately significant values of decrease were obtained, ranging from the center to the northeast of the sub-basin. Regarding the amplitude and frequency analysis, it was shown that in

Tecnología y ciencias del agua, ISSN 2007-2422, 16(1), 84-137. DOI: 10.24850/j-tyca-2025-01-03

both the first and second analysis periods (each lasting 30 years), the rainy season persists from May to October. However, there was a maximum reduction of 20 mm in precipitation in the month of May, as well as a decrease of 9 mm in the wettest month (July), between the two periods. May emerged as the warmest month for both maximum and mean temperatures, but its value decreased by 0.4 and 0.5 °C, respectively, in the second period. June and July are the warmest months for minimum temperature, and their values also showed a reduction of 0.5 °C from the first to the second period. It is worth noting that the second analysis period (1986-2015) witnessed an increase in maximum temperature values during the cooler season of the year (from July to February).

Despite the results obtained in the analysis of spatio-temporal trends and in the seasonal analysis of amplitude and frequency, the results of the analysis of the Köppen-Geiger climate categorization indicate that neither the precipitation conditions nor the temperature conditions of the second period have modified the type of climate present in the sub-basin, concluding that the climate has remained constant in the *Sila* river sub-basin in the last 60 years.

The results obtained were compared with the climate change scenarios, which indicate that the sub-basin will continue to have a temperate climate, with dry winters and hot summers (*Cwb*), under different climate change scenarios between 2000 and 2100 (Rubel & Kottek, 2010). Based on the aforementioned ideas, and using the available data between 1956 and 2015, we consider it probable that the behaviour of the analysed climatic elements (precipitation and temperature) remains relatively stable spatially and temporally in this sub-basin. As long as the current conditions in the sub-basin do not change drastically, it is likely that its climate will continue to be influenced by natural climatic variability; however, one must always keep in mind the conditions of global climate change.

The results obtained do not ensure the persistence of the current climate, which could be modified by the effects of human activity as indicated by the definition of climate change. Therefore, conservation actions are necessary to preserve the current and future state of the sub-basin. Finally, the results of the Köppen-Geiger climate classification could be compared with the Köppen-García climate classification for both periods, as it is a specific method for the climatic characteristics of the Mexican Republic. The results of the Köppen-García climate classification could reinforce the results obtained in this research or generate new lines of research. It is also recommended to expand the study area at the basin or hydrological region level, to find out how the climate has behaved at the basin level and/or if this behaviour depends on the local characteristics of the area being analysed.

Acknowledgments

The authors thank the National Council of Humanities, Science and Technology of Mexico, for financial support through a research grant to carry out this work, as well as the Autonomous University of the State of Mexico for providing access to the software for geospatial analysis and processing of the data used in this research.

References

Aawar, T., Khare, D., & Singh, L. (2019). Identification of the trend in precipitation and temperature over the Kabul River sub-basin: A case study of Afghanistan. *Modeling Earth Systems and Environment*, 5(4), 1377-1394. DOI: 10.1007/s40808-019-00597-9

Aparicio, F. (1992). *Fundamentos de hidrología de superficie*. México, DF, México: Limusa.

Astudillo-Sánchez, C. C., Villanueva-Díaz, J., Endara-Agramont, A. R., Nava-Bernal, G. E., & Gómez-Albores, M. A. (2017). Climatic variability at the treeline of Monte Tlaloc, Mexico: A dendrochronological approach. *Trees-Structure and Function*, 31(2), 441-453. DOI: 10.1007/s00468-016-1460-z

Baig, M. R., Shahfahad, Naikoo, M. W., Ansari, A. H., Ahmad, S., & Rahman, A. (2022). Spatio-temporal analysis of precipitation pattern and trend using standardized precipitation index and Mann-Kendall test in coastal Andhra Pradesh. *Modeling Earth Systems and Environment*, 8(2), 2733-2752. DOI: 10.1007/s40808-021-01262-w

Basarir, A., Arman, H., Hussein, S., Murad, A., Aldahan, A., & Al-Abri, M. A. (2018). Trend detection in annual temperature and precipitation using Mann-Kendall test. A case study to assess climate change in Abu Dhabi, United Arab Emirates. *Lecture Notes in Civil Engineering*, 7(Isbs 2017), 3-12. DOI: 10.1007/978-3-319-64349-6_1

Bedewi, A., & Kumar, A. (2018). Current and projected water demand and water availability estimates under climate change scenarios in the Weyib River basin in Bale mountainous area of Southeastern Ethiopia. *Theoretical and Applied Climatology*, 133(3-4), 727-735. DOI: 10.1007/s00704-017-2219-1

Bee, B. (2014). "Si no comemos tortilla, no vivimos": Women, climate change, and food security in central Mexico. *Agriculture and Human Values*, 31(4), 607-620. DOI: 10.1007/s10460-014-9503-9

Brassington, R. (1988). *Field hidrogeology*. Sydney, Australia: University Press and Halstead Press.

Brooks, K. N., Ffolliott, P. F., & Magner, J. A. (2013). *Hydrology and the Management of Watersheds*. Hoboken, USA: Wiley-Blackwell.

Campos, D. F. (1998). *Procesos del ciclo hidrológico*. San Luis Potosí, México: Universidad Potosina.

Campos, D. F. (2010). *Introducción a la hidrología urbana*. San Luis Potosí, México: Universidad Potosina.

CEDIPIEM, Consejo Estatal para el Desarrollo Integral de los Pueblos Indígenas. (2022). *Pueblos indígenas en el Estado de México*. Gobierno del Estado de México. Recovered from https://edomex.gob.mx/indigenas_edomex

Cepanaf, Comisión Estatal de Parques Naturales y de la Fauna. (2019). Programa de Manejo del Área Natural Protegida Parque Estatal “Santuario del Agua y Forestal Subcuenca Tributaria Arroyo Sila”. *Gaceta del Gobierno*.

Chow, Ven T., Maidment, D., & Mays, L. (1988). *Applied hydrology.* McGraw-Hill, New York, USA.

Colaborador. (2020). Aseguran en el Estado de México que es imposible que avionetas inhiban lluvias. *BRIO Agropecuario*. Recovered from https://brioagropecuario.com/2020/06/29/aseguran-en-el-estado-de-mexico-que-es-imposible-que-avionetas-inhiban-lluvias/

Colín, O. (2021). *Automatización de la clasificación climática de Koppen-Geiger en un SIG (Master's thesis)*. Universidad Autónoma del Estado de México, México.

Conagua, Comisión Nacional del Agua. (2023). *Consulta a la base de datos del REPDA*. Recovered from https://app.conagua.gob.mx/consultarepda.aspx

Conde, A. C., & López, J. (2016). *Variabilidad y cambio climático.* Instituto Nacional de Ecología y Cambio Climático. Recovered from https://biblioteca.semarnat.gob.mx/janium/Documentos/Ciga/Libros2013/CD002498.pdf

Da Silva, P., Araujo, M. A., & Fábio, F. (2022). Evaluation of InVEST's Water Ecosystem Service Models in a Brazilian Subtropical Basin. *Water*, 14(10). DOI: 10.3390/w14101559

Davie, T. (2008). *Fundamentals of hydrology*. Taylor y Francis. Recovered from http://books.google.com/books?hl=en&lr=&id=x0HfA6HJvogC&oi=fnd&pg=PP1&dq=Fundamentals+of+Hydrology&ots=fi3rcmkBRZ&sig=xXLEc2AGr243RS1Iqr6q66rbyFM

De Oliveira, L. E., Da Silva, J. R., De Meneses, K. C., Botega, G., De Lima, R. F., & Silva, C. T. (2020). Köppen-Geiger and Camargo climate classifications for the Midwest of Brasil. *Theoretical and Applied Climatology*, 142(3-4), 1133-1145. DOI: 10.1007/s00704-020-03358-2

Deng, C., Pisani, B., Hernández, H., & Li, Y. (2020). Assessing the impact of climate change on water resources in a semi-arid area in central Mexico using a SWAT model. *Boletín de la Sociedad Geológica Mexicana*. DOI: 10.1029/2008WR007615

Diaz, V., Bâ, K. M., Quentin, E., Ortiz, F. H., & Gama, L. (2015). Hydrological model to simulate daily flow in a basin with the help of a GIS. *Open Journal of Modern Hydrology*, 5(3), 58-67. DOI: 10.4236/ojmh.2015.53006

Engelbrecht, C. J., & Engelbrecht, F. A. (2016). Shifts in Köppen-Geiger climate zones over southern Africa in relation to key global temperature goals. *Theoretical and Applied Climatology*, 123(1-2), 247-261. DOI: 10.1007/s00704-014-1354-1

Fekadu, G., Biru, Z., & Mamo, G. (2019). Impacts of climate change on stream flow and water availability in Anger sub-basin, Nile Basin of Ethiopia. *Sustainable Water Resources Management*, 5(4), 1755-1764. DOI: 10.1007/s40899-019-00327-0

Gobierno de la República. (2014). *Programa especial de Cambio Climático. Plan Nacional de Desarrollo 2013-2018*. Mexico City, Mexico.

González-Celda, G., Ríos, N., Benegas-Negri, L., & Argotty-Benavides, F. (2021). Impacto del cambio climático y cambio de uso/cobertura de la tierra en la respuesta hidrológica y erosión hídrica en la subcuenca del río Quiscab. *Tecnología y ciencias del agua*. DOI: 10.24850/j-tyca-2021-06-09

Heano, J. (2006). *Introducción al manejo de cuencas hidrográficas*. Bogotá, Colombia: Universidad Santo Tomás.

Hutchinson, M. F., & Xu, T. (2013). *Anusplin version 4.4. User Guide. August*. Recovered from http://fennerschool.anu.edu.au/files/anusplin44.pdf

INECC, Instituto Nacional de Ecología y Cambio Climático. (2022). *Actualización de los escenarios de cambio climático para estudios de impactos, vulnerabilidad y adaptación*. Recovered from http://atlasclimatico.unam.mx:8578/AECC/servmapas

INEGI, Instituto Nacional de Estadística y Geografía. (2020). *Marco geoestadístico*. Recovered from https://www.inegi.org.mx/temas/mg/#Descargas

INEGI, Instituto Nacional de Estadística y Geografía. (2022). *Cobertura y uso de suelo*. Recovered from https://www.inegi.org.mx/

IPCC, Grupo Intergubernamental de Expertos sobre el Cambio Climático (2023). *Climate change 2023*. Recovered from https://www.unep.org/resources/report/climate-change-2023-synthesis-report

Jiang, R., Xie, J., Zhao, Y., He, H., & He, G. (2017). Spatiotemporal variability of extreme precipitation in Shaanxi province under climate change. *Theoretical and Applied Climatology*, 130(3-4), 831-845. DOI: 10.1007/s00704-016-1910-y

Karger, D. N., Conrad, O., Böhner, J., Kawohl, T., Kreft, H., Soria-Auza, R. W., Zimmermann, N. E., Linder, H. P., & Kessler, M. (2017). Climatologies at high resolution for the earth’s land surface areas. *Scientific Data*, 4, 1-20. DOI: 10.1038/sdata.2017.122

Krishnan, N., Prasanna, M. V., & Vijith, H. (2019). Statistical analysis of trends in monthly precipitation at the Limbang River Basin, Sarawak (NW Borneo), Malaysia. *Meteorology and Atmospheric Physics*, 131(4), 883-896. DOI: 10.1007/s00703-018-0611-8

Linsley, R., Kohler, M., & Paulhus, J. (1958). *Hydrology for engineers*. McGraw-Hill, New York, USA.

López, S., Expósito, J. L., Esteller, M. V., Gómez, M. A., Paredes, J., & Esquivel, J. M. (2021). Delineation of protection zones for springs in fractured volcanic media considering land use and climate change scenarios in central Mexico region. *Environmental Earth Sciences*. DOI: 10.1007/s12665-021-09662-y

Marques, R., Santos, C., Moreira, M., Corte-Real, J., Silva, V., & Medeiros, I. (2015). Rainfall and river flow trends using Mann-Kendall and Sen’s slope estimator statistical tests in the Cobres River basin. *Natural Hazards*, 77(2), 1205-1221. DOI: 10.1007/s11069-015-1644-7

McCuen, R. H. (1998). *Hydrologic Analysis and Design*. Pearson, Upper Saddle River, New Jersey, USA.

Minga, S. (2018). *Análisis de cambio del rendimiento hídrico actual y bajo escenarios climáticos futuros en la región sur del Ecuador (Master's thesis)*. Recovered from http://hdl.handle.net/20.500.11799/99126

Nandi, S., & Manne, J. R. (2020). Spatiotemporal analysis of water balance components and their projected changes in near-future under climate change over Sina Basin, India. *Water Resources Management*, 34(9), 2657-2675. DOI: 10.1007/s11269-020-02551-2

Naranjo, L., Glantz, M. H., Temirbekov, S., & Ramírez, I. J. (2018). El Niño and the Köppen-Geiger Classification: A Prototype concept and methodology for mapping impacts in Central America and the Circum-Caribbean. *International Journal of Disaster Risk Science*, 9(2), 224-236. DOI: 10.1007/s13753-018-0176-7

Ngoma, H., Wen, W., Ojara, M., & Ayugi, B. (2021). Assessing current and future spatiotemporal precipitation variability and trends over Uganda, East Africa, based on CHIRPS and regional climate model datasets. *Meteorology and Atmospheric Physics*, 133(3), 823-843. DOI: 10.1007/s00703-021-00784-3

Nigusie, A., & Wondimagegn, W. (2020). Assessment of hydrology and optimal water allocation under changing climate conditions: The case of Megech river sub basin reservoir, upper Blue Nile Basin, Ethiopia. *Modeling Earth Systems and Environment*, 7(4), 2629-2642. DOI: 10.1007/s40808-020-01024-0

Nonki, R. M., Lenouo, A., Lennard, C. J., & Tchawoua, C. (2019). Assessing climate change impacts on water resources in the Benue River Basin, Northern Cameroon. *Environmental Earth Sciences*, 78(20). DOI: 10.1007/s12665-019-8614-4

Nourani, V., Mehr, A. D., & Azad, N. (2018). Trend analysis of hydroclimatological variables in Urmia lake basin using hybrid wavelet Mann-Kendall and Şen tests. *Environmental Earth Sciences*, 77(5), 1-18. DOI: 10.1007/s12665-018-7390-x

Núñez-González, G. (2020). Analysis of the trends in precipitation and precipitation concentration in some climatological stations of Mexico from 1960 to 2010. *Natural Hazards*, 104(2), 1747-1761. DOI: 10.1007/s11069-020-04244-w

OMM, Organización Meteorológica Mundial. (2018). *Guía de prácticas climatológicas*. Ginebra, Suiza: World Meteorological Organization.

OMM, Organización Meteorológica Mundial. (2022). *Organización Meteorológica Mundial. Preguntas frecuentes. Clima*. Recovered from https://public.wmo.int/es/preguntas-frecuentes-clima

Pandey, B. K., Khare, D., Kawasaki, A., & Mishra, P. K. (2019). Climate change impact assessment on blue and green water by coupling of representative CMIP5 climate models with physical based hydrological model. *Water Resources Management*. DOI: 10.1007/s11269-018-2093-3

Pilares, I., Montalvo, N., Mejía, A., Guevara-Perez, E., Fano, G., & Alfaro, R. (2018). Evaluation of water availability in the Cabanillas river basin of the Peruvian Altiplano under regionalized climatic scenario. *Ingenieria UC*, 25(2), 307-319.

Rahimi, J., Laux, P., & Khalili, A. (2020). Assessment of climate change over Iran: CMIP5 results and their presentation in terms of Köppen-Geiger climate zones. *Theoretical and Applied Climatology*, 141(1-2), 183-199. DOI: 10.1007/s00704-020-03190-8

Rodríguez, A. (2022). Disputas por agua entre el Complejo Industrial Pastejé y Los Reyes Jocotitlán, Estado de México (México): espacialización industrial e hídrica a escala regional. *Secuencia*, 114. DOI: 10.18234/secuencia.v0i114.1917

Ronald, J. (2016). *TerrSet. Geospatial Monitoring and Modeling System.* Clark University, Massachusetts, USA. Recovered from *https://clarklabs.org/terrset/*

Rubel, F., & Kottek, M. (2010). Observed and projected climate shifts 1901-2100 depicted by world maps of the Köppen-Geiger climate classification. *Meteorologische Zeitschrift*, 19(2), 135-141. DOI: 10.1127/0941-2948/2010/0430

Ruman, A. (2020). Modelling climate types in South Pannonian Basin, Serbia by applying the Köppen-Geiger climate classification. *Modeling Earth Systems and Environment*, 6(3), 1303-1313. DOI: 10.1007/s40808-020-00773-2

Shaw, E. M., Beven, K. J., Chappell, N. A., & Lamb, R. (2011). *Hydrology in practice*. Taylor & Francis. DOI: 10.1201/9781315274904

U.S. Army Corps of Engineers. (2005). Mann-Kendall analysis for the Fort Ord Site. *HydroGeoLogic, Inc.*, 1-7. Recovered from https://www.statisticshowto.com/wp-content/uploads/2016/08/Mann-Kendall-Analysis-1.pdf

UN, United Nations. (1992). *United Nations Framework Convention on Climate Change*. 62220. New York, USA: United Nations.

Vázquez-Ochoa, L. A., Correa-Sandoval, A., Vargas-Castilleja, R., Vázquez-Sauceda, M., & Rodríguez-Castro, J. H. (2021). Modelo hidrológico, calidad del agua y cambio climático: soporte para la gestión hídrica de la cuenca del río Soto la Marina. *CienciaUAT*. DOI: 10.29059/cienciauat.v16i1.1498

Viessman, W., & Lewis, G. (1995). *Introduction to hydrology*. Prentice Hall, Upper Saddle River, New Jersey, USA.

Wang, Y., Wang, X., Li, C., Wu, F., & Yang, Z. (2015). Spatiotemporal analysis of temperature trends under climate change in the source region of the Yellow River, China. *Theoretical and Applied Climatology*, 119(1-2), 123-133. DOI: 10.1007/s00704-014-1112-4

Yanming, Z., Jun, W., & Xinhua, W. (2011). Study on the change trend of precipitation and temperature in kunming city based on Mann-Kendall analysis. *Advances in Intelligent and Soft Computing*, 119, 505-513. DOI: 10.1007/978-3-642-25538-0_71

Zeroual, A., Assani, A. A., Meddi, M., & Alkama, R. (2019). Assessment of climate change in Algeria from 1951 to 2098 using the Köppen–Geiger climate classification scheme. *Climate Dynamics*, 52(1-2), 227-243. DOI: 10.1007/s00382-018-4128-0